Letter

Demonstration of high sensitivity of microwave-induced resistance oscillations to circular polarization

M. L. Savchenko,[1,2] A. Shuvaev,[1] I. A. Dmitriev,[3] S. D. Ganichev,[3] Z. D. Kvon,[2,4] and A. Pimenov[1]

[1]*Institute of Solid State Physics, Vienna University of Technology, 1040 Vienna, Austria*

[2]*Rzhanov Institute of Semiconductor Physics, 630090 Novosibirsk, Russia*

[3]*Terahertz Center, University of Regensburg, 93040 Regensburg, Germany*

[4]*Novosibirsk State University, 630090 Novosibirsk, Russia*

(Received 17 June 2022; revised 26 August 2022; accepted 5 October 2022; published 14 October 2022)

We demonstrate that the long-debated immunity of the microwave-induced resistance oscillations (MIRO) to the sense of circular polarization is in fact not an inherent property of this phenomenon in solid-state two-dimensional electron systems (2DES): We detect an up to 30 times larger MIRO signal for the cyclotron resonance (CR) active helicity, fully consistent with the concurrently measured transmission and the deduced CR shape of the Drude absorption. Using a 2DES as a sensitive sensor of the actual polarization state, we further study extrinsic near-field effects capable of producing an apparent immunity of the photoresponse.

DOI: 10.1103/PhysRevB.106.L161408

Introduction. In the last two decades, studies of high-mobility two-dimensional electron systems (2DES) in a weakly quantizing magnetic field have given access to a family of fascinating interrelated magneto-oscillation phenomena reflecting various spatial and spectral resonances that emerge at high Landau levels under application of static and/or alternating (microwave or terahertz) electric fields [1–17]. Experimental research in a growing number of high-mobility 2DES [18–28] and various conditions have been accompanied by theoretical developments which provided new insights into the interplay of Landau quantization, disorder, and interactions in electron kinetics in both weakly and strongly nonequilibrium regimes of magnetotransport [1,29–45]. These studies have been largely motivated by the discovery of giant microwave-induced resistance oscillations (MIRO) [2], magneto-oscillations of photoresistance controlled by the ratio of the microwave and cyclotron frequencies, as well as the radiation-induced zero-resistance states [3–5] that emerge at deep minima of MIRO and represent a rare example of electric domain instability associated with negative absolute conductivity in strongly driven 2DES.

Despite much progress in unified understanding of the above phenomena, the developed theory of MIRO is considered inadequate in view of the reported puzzling insensitivity of MIRO to helicity of the incoming radiation [11,16]. The microscopic theory [1] predicts a strong asymmetry of MIRO with respect to the polarity of the magnetic field B, applied perpendicular to the 2DES plane, in the case of circular polarization of incident radiation. According to this theory, at low radiation intensity I the photoresistance, $\delta R(B) = IA^{\mathrm{D}}(B)f(|B|)$, can be represented as a product of the quasiclassical Drude absorptance, $A^{\mathrm{D}}(B)$, which should be strongly enhanced near the cyclotron resonance (CR) either at positive or negative $B = \eta B_{\mathrm{CR}}$ depending on the helicity $\eta = \pm 1$ of the incoming wave, and a mechanism-dependent function $f(|B|)$ which describes the magneto-oscillations and is insensitive to the sign of B or η. In sharp contrast to the expected pronounced B asymmetry,

$$\delta R(B)/\delta R(-B) = A^{\mathrm{D}}(B)/A^{\mathrm{D}}(-B), \tag{1}$$

the experiments revealed completely symmetric [11] or weakly asymmetric [16] magneto-oscillations in the photoresistance. At the same time, these experiments demonstrated a strongly asymmetric transmittance $T(B)$ through the 2DES, with a single dip at $B = \eta B_{\mathrm{CR}}$, thus apparently confirming the validity of the quasiclassical theory behind interrelated $A(B)$ and $T(B)$, as well as the purity of the circular polarization of the incoming wave.

Here we provide a counterexample of a GaAs-based 2DES that exhibits an unmitigated helicity dependence in both transmittance and MIRO in full agreement with Eq. (1). We thus prove that, contrary to a widespread view, the long-debated polarization immunity is not an inherent property of MIRO in solid-state 2DES but rather reflects certain yet unknown peculiarities of technological design and corresponding realization of disorder in particular structures. We also establish the necessary conditions to avoid extrinsic electrodynamic effects capable of producing an apparent polarization immunity of MIRO.

Methods. Our simultaneous transmittance and photoresistance measurements [see Fig. 1(a)] were carried out on a heterostructure containing a 2DES in a selectively doped 16-nm GaAs quantum well with AlAs/GaAs superlattice barriers grown by molecular beam epitaxy [46–50]. The lateral size of the van der Pauw sample was 10×10 mm^2, with ohmic Ge/Au/Ni/Au contacts at the corners. The electron density and mobility extracted from magnetotransport measurements were $n = 7.0 \times 10^{11}$ cm^{-2} and $\mu = 1.0 \times 10^6$ cm^2 V^{-1} s^{-1}. The sample was irradiated from the substrate side through a 10-mm absorber aperture (Fig. 1) or circular metallic apertures of varying diameter (Fig. 2); for details, see

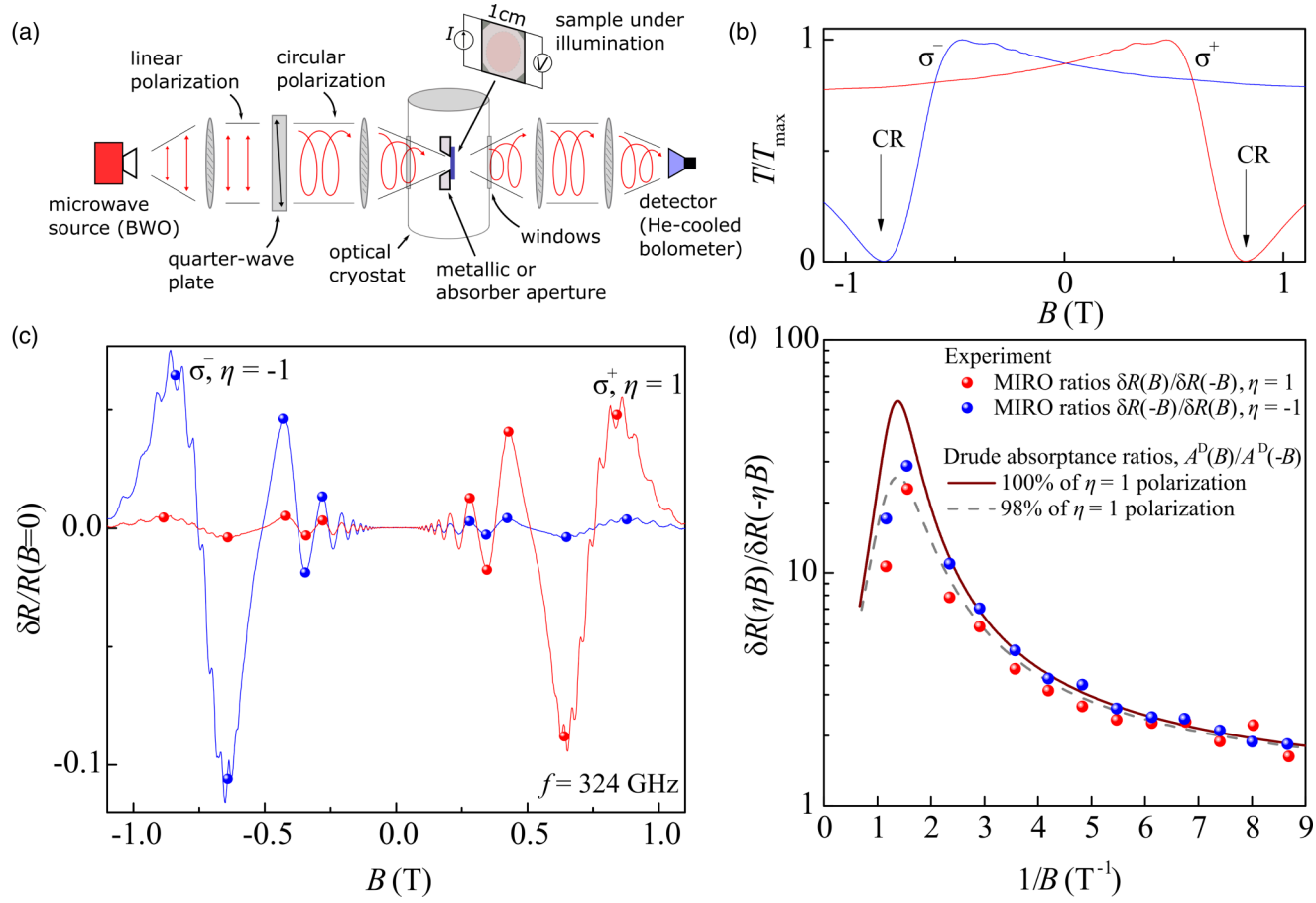

FIG. 1. (a) Scheme of the experiment (the irradiated sample area is highlighted). (b) and (c) Magnetic field dependences of the transmittance $T(B)$, normalized to its maximum value $T_{\max}$ (b), and MIRO in the longitudinal photoresistance δR, normalized to the zero-field dark resistance $R(B=0)$ (c), for the right-hand (σ^+, $\eta=1$, red) and left-hand (σ^-, $\eta=-1$, blue) circularly polarized radiation. (d) The ratios $\delta R(\eta B)/\delta R(-\eta B)$ at extrema of the MIRO signals [spheres in (c)] illustrating the asymmetry of MIRO between the CR-active and CR-passive polarities of B for $\eta=1$ (red spheres) and $\eta=-1$ (blue spheres). The solid curve shows the ratio $A^{\mathrm{D}}(B)/A^{\mathrm{D}}(-B)$ of the Drude absorption calculated for $\eta=1$ using parameters extracted from the dark transport measurements and transmission $T(B)$ shown in (b) and (c).

Supplemental Material [46]. Backward-wave oscillators were used as stable sources of normally incident continuous monochromatic radiation with frequency $f=\omega/2\pi$ in the range between 50 and 500 GHz. A split-coil superconducting magnet provided a magnetic field oriented perpendicular to the sample surface. The photoresistance δR (the difference of the resistance signals in the presence and absence of irradiation) was measured using the double-modulation technique [46]. In parallel with the photoresistance, the transmittance through the sample was measured using a liquid-He-cooled bolometer. All presented results were obtained at a temperature of 3.7 K.

Helicity dependence of MIRO, transmittance, and absorptance. Figure 1 shows representative examples of simultaneously measured transmittance $T(B)$ and photoresistance $\delta R(B)$, recorded for both helicities $\eta=1$ and $\eta=-1$ of $f=\omega/2\pi=324$ GHz circularly polarized radiation. The transmittance traces in Fig. 1(b) display strong dips at the CRs, $B=\eta B_{\mathrm{CR}}$, marked by arrows. The absence of any features at opposite $B=-\eta B_{\mathrm{CR}}$ confirms a high degree of the circular polarization in the transmitted signal. The photoresistance $\delta R(B)$ in Fig. 1(c) shows pronounced MIRO governed by the ratio $\omega/\omega_{\mathrm{c}}$ of the radiation and cyclotron frequencies. In sharp contrast to previous reports [11,16], our results reveal a high asymmetry of MIRO with respect to polarity of B which inverts with the change in radiation helicity η. This is one of our central observations, which unequivocally demonstrates that the long-debated polarization immunity is not an inherent property of MIRO in solid-state 2DES.

Moreover, we find an excellent quantitative agreement between the shape of CR in measured $T(B)$ and the B asymmetry of the MIRO signal, in full accordance with Eq. (1). This agreement is illustrated in Fig. 1(d), where we plot ratios $\delta R(\eta B)/\delta R(-\eta B)$ of the MIRO signal between CR-active and CR-passive polarities of B, for both helicities. Here we use values of δR at the opposite-lying MIRO extrema marked by spheres in Fig. 1(c). It is seen that the asymmetry is strongly enhanced in the region of CR reaching values of $\sim$30 for the main MIRO extrema around $\omega=\omega_{\mathrm{c}}$. Solid and dashed curves show the corresponding ratio $A^{\mathrm{D}}(B)/A^{\mathrm{D}}(-B)$ of the Drude absorption calculated using parameters extracted from the shape of $T(B)$ in Fig. 1(b), for 100% right circular polarization and for a 98% to 2% mixture of right and left polarizations, respectively. An almost perfect agreement with Eq. (1) demonstrates an ultimate sensitivity of MIRO to circular polarization. It is important to emphasize that this comparison, detailed

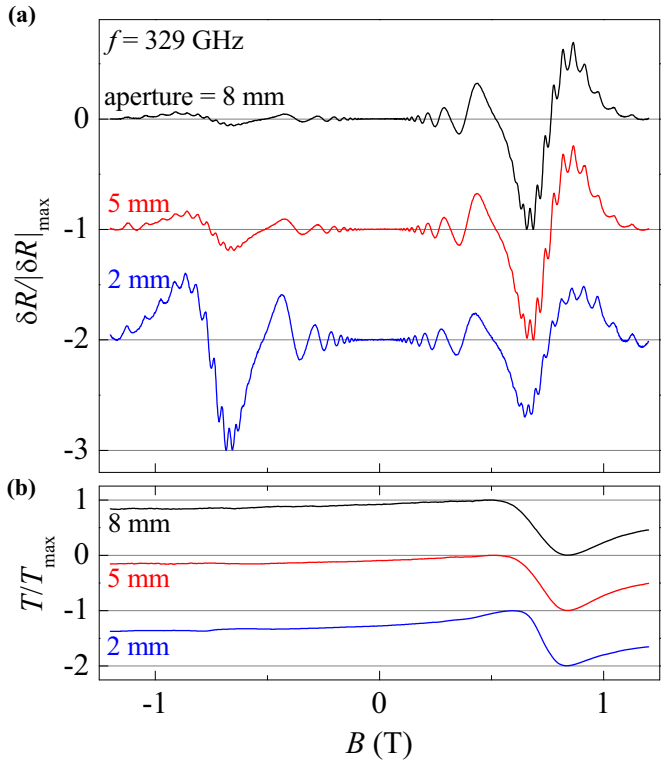

FIG. 2. (a) MIRO signal measured at $f = 329$ GHz ($\lambda \approx 0.9$ mm) using metallic apertures with different diameters as indicated. (b) Normalized transmission through the sample measured *in situ*.

below, does not assume any specific microscopic mechanism of MIRO. It rather establishes that the polarization dependences of MIRO and of the Drude absorption are the same.

Modeling of transmittance and absorptance. As detailed in the Supplemental Material [46], the shape of $T(B)$ can be well reproduced using the standard expression $T(B) = 4/|s_1(1 + Z_0\sigma_\eta) + s_2|^2$, with the complex dynamic conductivity $\sigma_\eta = \sigma_{xx} + i\eta\sigma_{yx}$ of the 2DES taken in the classical Drude form, $\sigma_\eta^{\rm D} = e^2 n/(\mu^{-1} - iB_{\rm CR} + i\eta B)$, and with two complex parameters $s_{1,2} = \cos\phi - in_r^{\mp 1}\sin\phi$ describing the Fabry-Pérot interference due to multiple reflections in the GaAs substrate [1,28,51–53]. Here, the interference phase $2\phi = 4\pi w/\lambda_r$ is given by the ratio of the sample thickness w and the wavelength $\lambda_r = c/fn_r$, n_r is the refractive index of the substrate, and $Z_0 \approx 377\ \Omega$ is the impedance of free space. The resulting Drude transmittance $T^{\rm D}$ and Drude absorptance, $A^{\rm D} = Z_0 T^{\rm D} {\rm Re}\,\sigma_\eta^{\rm D}$, are given by

$$T^{\rm D}(B) = |\alpha|^2 \left| 1 - \frac{\beta}{\mu^{-1} + \beta - iB_{\rm CR} + i\eta B} \right|^2, \qquad (2)$$

$$A^{\rm D}(B) = \frac{Z_0 |\alpha|^2 e^2 n/\mu}{|\mu^{-1} + \beta - iB_{\rm CR} + i\eta B|^2}, \qquad (3)$$

where $\alpha = 2/(s_1 + s_2)$ and $\beta = enZ_0/(1 + s_1/s_2)$. The shape of measured $T(B)$ in Fig. 1 is well reproduced by Eq. (2) using $\mu^{-1} = 0.01$ T extracted from magnetotransport measurements, $B_{\rm CR} = m_{\rm CR}\omega/e = 0.83$ T corresponding to the cyclotron mass $m_{\rm CR} = 0.071 m_0$, and $\beta = (0.183 + i\,0.127)$ T [46]. On top of smooth Drude transmittance, our high-resolution measurements are able to resolve the weak quantum $\omega/\omega_{\rm c}$ oscillations studied in Ref. [54]. The extracted parameters are used in the calculated ratios $A^{\rm D}(B)/A^{\rm D}(-B)$ in Fig. 1(d), which establish the validity of Eq. (1).

Aperture dependence of the polarization-sensitive measurements. Having established that the intrinsic helicity dependence of MIRO is ultimately strong in the sense that it accurately follows the helicity dependence of transmittance and deduced Drude absorption, we have further studied extrinsic near-field effects capable of producing an apparent immunity of the photoresponse. Here, we used the GaAs sample as a sensitive near-field sensor of the actual polarization state and studied the effect of metallic apertures that are typically used to avoid illumination of the contacts and sample edges in this type of experiment. Figure 2 shows the B dependencies of the photoresistance [Fig. 2(a)] and transmittance [Fig. 2(b)] measured at 329 GHz ($\lambda \approx 0.9$ mm) with varying diameter of the aperture. Figure 2(a) demonstrates that the MIRO asymmetry strongly depends on the diameter when other experimental parameters are kept unchanged. The MIRO ratio $\delta R(B)/\delta R(-B)$ is the largest for an 8-mm aperture and tends towards unity for diaphragms smaller than the estimated size of the focal spot of about 4 mm. In contrast, the transmittance signal in Fig. 2(b) does not considerably change for different apertures.

We explain such behavior as follows: The MIRO signal is sensitive to the polarization of the local electromagnetic field. If the aperture size is too small such that the radiation interacts with the metallic edges, then the local polarization in the nearby 2DES will be linear regardless of the incident degree of the circular polarization. This follows from the boundary conditions requiring that the E field can only have a normal component at the metal surface [55]. Therefore the radiation that interacts with the metal aperture results in a distortion of the local polarization and, consequently, of the detected photoresistance signal reflecting the local absorption.

The appearance of a local linearly polarized electric field can be understood considering a circularly polarized wave irradiating a circular metallic waveguide; see Supplemental Material [46] for details. The distribution of local circularly-rotating electric fields that fulfill the boundary conditions is given by

$$E_+ = -iEJ_0(k_r r), \quad E_- = -ie^{2i\varphi}EJ_2(k_r r). \qquad (4)$$

Here, J_n are Bessel functions of the nth order, k_r is the radial wave vector of the lowest propagating mode in a circular waveguide, $E_\pm$ are right- and left-rotating circular fields, and E is the amplitude of the incident electric field. The distributions of the circular components E_+ and E_- are shown in Figs. 3(a) and 3(b), respectively. The amplitude of $E_+ \sim J_0(k_r r)$ is rotationally symmetric across the waveguide with a flat maximum in the middle. Obviously, this is the same polarization as that of the incident circularly polarized beam. In contrast, the $E_- \sim J_2(k_r r)$ is zero in the middle of the waveguide and changes sign four times along the wall of the waveguide.

According to the Huygens-Fresnel principle the amplitude of the transmitted wave is given by the sum of secondary sources from all points on the wave front. After integration of the E_- fields, negative and positive regions cancel each

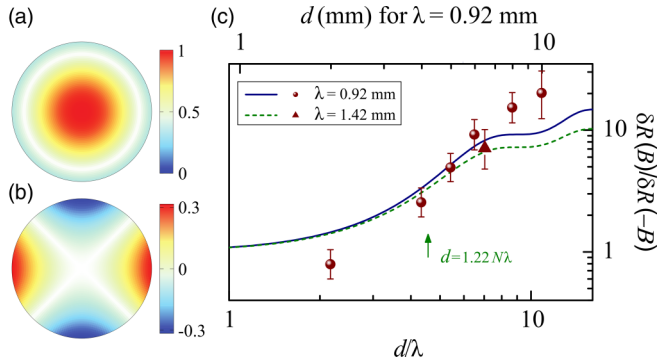

FIG. 3. (a) and (b) Circular decomposition of the electric field (4) in the waveguide: the incident E_+ (a) and distorted E_- (b) helicity components of the near field reaching the 2DES. (c) Symbols: Maximal MIRO ratios in experiments with varying diameters of the diaphragm. Curves are calculated using Eqs. (1), (3), and (5) for $\lambda = 0.92$ mm (solid curve) and $\lambda = 1.42$ mm (dashed curve); see text for details. Arrow: the diffraction spot $d = 1.22N\lambda$.

other. Thereby, the distorted polarization is absent in the far field and produces no signal at the detector. This is the reason why all curves in Fig. 2(b) show only one well-defined CR. In contrast to the transmittance, the absorbed power and MIRO are proportional to the square of the local near field. Therefore the response to the distorted polarization does not vanish in the resistivity signal.

While the field distribution (4) of the lowest modes readily provides a qualitative explanation of our results, in order to describe the full dependence of the MIRO asymmetry on the aperture size the boundary problem has to be solved numerically taking into account all higher-order modes. Instead, here we loosely model this dependence assuming that the integrated intensities of the parts of the beam falling inside and outside the diaphragm provide a rough estimate for the relative weight of active ($I_A = |E_+|^2$) and passive ($I_P = |E_-|^2$) circular components in the 2DES. The radial distribution of the radiation intensity in the focus of the lens is given by [56]

$$I(x)/I(0) = 2|J_1(x)/x|^2, \tag{5}$$

where $x = \pi d/2N\lambda$ is the normalized aperture diameter and $N = F/D \approx 3.6$ is the f number of the focusing lens with diameter $D \approx 4.5$ cm and focal length $F \approx 16$ cm.

Model curves in Fig. 3(c) are calculated using the relation (1) between the MIRO and absorption ratios and Eq. (3) for the absorption. In the latter, the intensities I_A and I_P are obtained from Eq. (5) as outlined above. In the limit $d \gg \lambda$ (100% active polarization), the maximal absorption ratio equals 50 for $f = 329$ GHz (solid curve, $\lambda = 0.92$ mm) and 32 for $f = 211$ GHz (dashed curve, $\lambda = 1.42$ mm). The difference originates from the frequency dependence of the absorption in Eq. (3). We observe that the curves yield reasonable fits to the experimental points. In particular, the MIRO ratio tends to unity for apertures below the diffraction spot $d = 1.22N\lambda$ indicated by the arrow. Under these conditions one should expect a substantial contribution of the near-field wave component with the opposite helicity.

Discussion. Our results demonstrate that the long-debated polarization immunity is not an inherent intrinsic property of MIRO in solid-state 2DES: (i) We detect strong intrinsic helicity dependence of MIRO that accurately follows the regular CR in the Drude absorption, and (ii) we show that extrinsic factors deteriorating the polarization state of the radiation can be avoided using sufficiently large samples and apertures. On the other hand, very recent experiments [57], where several similarly large samples were studied at terahertz frequencies, revealed a helicity immunity of the resonant photoresponse which directly measures the intraband CR absorption via heating of the 2DES. This clearly shows that the helicity immunity problem remains and, moreover, has a fundamental origin not related to MIRO. The experiments in Ref. [57] indicate that in a certain class of 2DES the internal high-frequency response of electrons to a uniform external field should be essentially nonuniform, producing an intrinsic helicity distortion of the near field in the vicinity of individual strong scattering centers or inhomogeneities, similar to the distortions of extrinsic origin studied in this Research Letter. Altogether, these insights into the essence of the helicity immunity problem open an interesting research direction deserving further experimental and theoretical efforts.

Conclusions. In the subterahertz frequency range we observed MIRO in a GaAs/AlGaAs 2DES that are ultimately sensitive to the helicity of circularly polarized radiation. The helicity dependence accurately follows that of the Drude absorption, in full agreement with natural expectations. Moreover, we demonstrate that observation of intrinsic polarization dependence requires large sample sizes and large apertures. Otherwise, the near field reaching the 2DES has a significant component of the opposite helicity, which does not affect the transmittance measured in the far field but essentially changes the asymmetry of the MIRO signal leading to apparent polarization immunity. Our results provide the opportunity to reliably test other systems potentially featuring an intriguing intrinsic polarization immunity of the photoresponse.

The authors thank E. Mönch, D. A. Kozlov, D. G. Polyakov, and J. H. Smet for valuable discussions. We are grateful to A. K. Bakarov and A. A. Bykov for providing high-quality GaAs/AlGaAs samples. We acknowledge the financial support of the Austrian Science Funds (I 3456-N27 and I 5539-N) and of the German Research Foundation (Deutsche Forschungsgemeinschaft) via Grant No. DM 1/5-1 (I.A.D.) and via subproject A04 of Project No. 314695032 - SFB 1277 (S.D.G.).

[1] I. A. Dmitriev, A. D. Mirlin, D. G. Polyakov, and M. A. Zudov, Nonequilibrium phenomena in high Landau levels, Rev. Mod. Phys. **84**, 1709 (2012).

[2] M. A. Zudov, R. R. Du, J. A. Simmons, and J. L. Reno, Shubnikov–de Haas-like oscillations in millimeterwave photoconductivity in a high-mobility two-dimensional electron gas, Phys. Rev. B **64**, 201311(R) (2001).

[3] R. G. Mani, J. H. Smet, K. von Klitzing, V. Narayanamurti, W. B. Johnson, and V. Umansky, Zero-resistance states induced by electromagnetic-wave excitation in

GaAs/AlGaAs heterostructures, Nature (London) **420**, 646 (2002).

[4] M. A. Zudov, R. R. Du, L. N. Pfeiffer, and K. W. West, Evidence for a New Dissipationless Effect in 2D Electronic Transport, Phys. Rev. Lett. **90**, 046807 (2003).

[5] C. L. Yang, M. A. Zudov, T. A. Knuuttila, R. R. Du, L. N. Pfeiffer, and K. W. West, Observation of Microwave-Induced Zero-Conductance State in Corbino Rings of a Two-Dimensional Electron System, Phys. Rev. Lett. **91**, 096803 (2003).

[6] M. A. Zudov, I. V. Ponomarev, A. L. Efros, R. R. Du, J. A. Simmons, and J. L. Reno, New Class of Magnetoresistance Oscillations: Interaction of a Two-Dimensional Electron Gas with Leaky Interface Phonons, Phys. Rev. Lett. **86**, 3614 (2001).

[7] C. L. Yang, J. Zhang, R. R. Du, J. A. Simmons, and J. L. Reno, Zener Tunneling Between Landau Orbits in a High-Mobility Two-Dimensional Electron Gas, Phys. Rev. Lett. **89**, 076801 (2002).

[8] W. Zhang, M. A. Zudov, L. N. Pfeiffer, and K. W. West, Resonant Phonon Scattering in Quantum Hall Systems Driven by dc Electric Fields, Phys. Rev. Lett. **100**, 036805 (2008).

[9] W. Zhang, M. A. Zudov, L. N. Pfeiffer, and K. W. West, Resistance Oscillations in Two-Dimensional Electron Systems Induced by Both ac and dc Fields, Phys. Rev. Lett. **98**, 106804 (2007).

[10] S. Wiedmann, G. M. Gusev, O. E. Raichev, A. K. Bakarov, and J. C. Portal, Microwave Zero-Resistance States in a Bilayer Electron System, Phys. Rev. Lett. **105**, 026804 (2010).

[11] J. H. Smet, B. Gorshunov, C. Jiang, L. Pfeiffer, K. West, V. Umansky, M. Dressel, R. Meisels, F. Kuchar, and K. von Klitzing, Circular-Polarization-Dependent Study of the Microwave Photoconductivity in a Two-Dimensional Electron System, Phys. Rev. Lett. **95**, 116804 (2005).

[12] S. I. Dorozhkin, L. Pfeiffer, K. West, K. von Klitzing, and J. H. Smet, Random telegraph photosignals in a microwave-exposed two-dimensional electron system, Nat. Phys. **7**, 336 (2011).

[13] A. A. Bykov, I. V. Marchishin, A. V. Goran, and D. V. Dmitriev, Microwave induced zero-conductance state in a Corbino geometry two-dimensional electron gas with capacitive contacts, Appl. Phys. Lett. **97**, 082107 (2010).

[14] A. D. Levin, Z. S. Momtaz, G. M. Gusev, O. E. Raichev, and A. K. Bakarov, Microwave-Induced Magneto-Oscillations and Signatures of Zero-Resistance States in Phonon-Drag Voltage in Two-Dimensional Electron Systems, Phys. Rev. Lett. **115**, 206801 (2015).

[15] S. I. Dorozhkin, A. A. Kapustin, V. Umansky, K. von Klitzing, and J. H. Smet, Microwave-Induced Oscillations in Magnetocapacitance: Direct Evidence for Nonequilibrium Occupation of Electronic States, Phys. Rev. Lett. **117**, 176801 (2016).

[16] T. Herrmann, I. A. Dmitriev, D. A. Kozlov, M. Schneider, B. Jentzsch, Z. D. Kvon, P. Olbrich, V. V. Bel'kov, A. Bayer, D. Schuh, D. Bougeard, T. Kuczmik, M. Oltscher, D. Weiss, and S. D. Ganichev, Analog of microwave-induced resistance oscillations induced in GaAs heterostructures by terahertz radiation, Phys. Rev. B **94**, 081301(R) (2016).

[17] Q. Shi, M. A. Zudov, I. A. Dmitriev, K. W. Baldwin, L. N. Pfeiffer, and K. W. West, Fine structure of high-power microwave-induced resistance oscillations, Phys. Rev. B **95**, 041403(R) (2017).

[18] D. Konstantinov, Yu. Monarkha, and K. Kono, Effect of Coulomb Interaction on Microwave-Induced Magnetoconductivity Oscillations of Surface Electrons on Liquid Helium, Phys. Rev. Lett. **111**, 266802 (2013).

[19] M. A. Zudov, O. A. Mironov, Q. A. Ebner, P. D. Martin, Q. Shi, and D. R. Leadley, Observation of microwave-induced resistance oscillations in a high-mobility two-dimensional hole gas in a strained quantum well, Phys. Rev. B **89**, 125401 (2014).

[20] D. F. Kärcher, A. V. Shchepetilnikov, Yu. A. Nefyodov, J. Falson, I. A. Dmitriev, Y. Kozuka, D. Maryenko, A. Tsukazaki, S. I. Dorozhkin, I. V. Kukushkin, M. Kawasaki, and J. H. Smet, Observation of microwave induced resistance and photovoltage oscillations in MgZnO/ZnO heterostructures, Phys. Rev. B **93**, 041410(R) (2016).

[21] R. Yamashiro, L. V. Abdurakhimov, A. O. Badrutdinov, Yu. P. Monarkha, and D. Konstantinov, Photoconductivity Response at Cyclotron-Resonance Harmonics in a Nondegenerate Two-Dimensional Electron Gas on Liquid Helium, Phys. Rev. Lett. **115**, 256802 (2015).

[22] A. A. Zadorozhko, Yu. P. Monarkha, and D. Konstantinov, Circular-Polarization-Dependent Study of Microwave-Induced Conductivity Oscillations in a Two-Dimensional Electron Gas on Liquid Helium, Phys. Rev. Lett. **120**, 046802 (2018).

[23] M. Otteneder, I. A. Dmitriev, S. Candussio, M. L. Savchenko, D. A. Kozlov, V. V. Bel'kov, Z. D. Kvon, N. N. Mikhailov, S. A. Dvoretsky, and S. D. Ganichev, Sign-alternating photoconductivity and magnetoresistance oscillations induced by terahertz radiation in HgTe quantum wells, Phys. Rev. B **98**, 245304 (2018).

[24] B. Friess, I. A. Dmitriev, V. Umansky, L. Pfeiffer, K. West, K. von Klitzing, and J. H. Smet, Acoustoelectric Study of Microwave-Induced Current Domains, Phys. Rev. Lett. **124**, 117601 (2020).

[25] D. Tabrea, I. A. Dmitriev, S. I. Dorozhkin, B. P. Gorshunov, A. V. Boris, Y. Kozuka, A. Tsukazaki, M. Kawasaki, K. von Klitzing, and J. Falson, Microwave response of interacting oxide two-dimensional electron systems, Phys. Rev. B **102**, 115432 (2020).

[26] E. Mönch, D. A. Bandurin, I. A. Dmitriev, I. Y. Phinney, I. Yahniuk, T. Taniguchi, K. Watanabe, P. Jarillo-Herrero, and S. D. Ganichev, Observation of terahertz-induced magnetooscillations in graphene, Nano Lett. **20**, 5943 (2020).

[27] P. Kumaravadivel, M. T. Greenaway, D. Perello, A. Berdyugin, J. Birkbeck, J. Wengraf, S. Liu, J. H. Edgar, A. K. Geim, L. Eaves, and R. Krishna Kumar, Strong magnetophonon oscillations in extra-large graphene, Nat. Commun. **10**, 3334 (2019).

[28] M. L. Savchenko, M. Otteneder, I. A. Dmitriev, N. N. Mikhailov, Z. D. Kvon, and S. D. Ganichev, Terahertz photoresistivity of a high-mobility 3D topological insulator based on a strained HgTe film, Appl. Phys. Lett. **117**, 201103 (2020).

[29] V. I. Ryzhii, Photoconductivity characteristics in thin films subjected to crossed electric and magnetic fields, Sov. Phys. Solid State **11**, 2078 (1970).

[30] A. C. Durst, S. Sachdev, N. Read, and S. M. Girvin, Radiation-Induced Magnetoresistance Oscillations in a 2D Electron Gas, Phys. Rev. Lett. **91**, 086803 (2003).

[31] I. A. Dmitriev, A. D. Mirlin, and D. G. Polyakov, Cyclotron-Resonance Harmonics in the ac Response of a 2D Electron Gas with Smooth Disorder, Phys. Rev. Lett. **91**, 226802 (2003).

[32] A. V. Andreev, I. L. Aleiner, and A. J. Millis, Dynamical Symmetry Breaking as the Origin of the Zero-dc-Resistance State in an ac-Driven System, Phys. Rev. Lett. **91**, 056803 (2003).

[33] M. G. Vavilov and I. L. Aleiner, Magnetotransport in a two-dimensional electron gas at large filling factors, Phys. Rev. B **69**, 035303 (2004).

[34] I. A. Dmitriev, M. G. Vavilov, I. L. Aleiner, A. D. Mirlin, and D. G. Polyakov, Theory of microwave-induced oscillations in the magnetoconductivity of a two-dimensional electron gas, Phys. Rev. B **71**, 115316 (2005).

[35] M. G. Vavilov, I. L. Aleiner, and L. I. Glazman, Nonlinear resistivity of a two-dimensional electron gas in a magnetic field, Phys. Rev. B **76**, 115331 (2007).

[36] I. A. Dmitriev, M. Khodas, A. D. Mirlin, D. G. Polyakov, and M. G. Vavilov, Mechanisms of the microwave photoconductivity in two-dimensional electron systems with mixed disorder, Phys. Rev. B **80**, 165327 (2009).

[37] O. E. Raichev, Magnetic oscillations of resistivity and absorption of radiation in quantum wells with two populated subbands, Phys. Rev. B **78**, 125304 (2008).

[38] Y. Monarkha and D. Konstantinov, Magneto-oscillations and anomalous current states in a photoexcited electron gas on liquid helium, J. Low Temp. Phys. **197**, 208 (2019).

[39] I. A. Dmitriev, Self-oscillations and noise-induced flips of spontaneous electric field in microwave-induced zero resistance state, Europhys. Lett. **126**, 57004 (2019).

[40] M. T. Greenaway, R. Krishna Kumar, P. Kumaravadivel, A. K. Geim, and L. Eaves, Magnetophonon spectroscopy of Dirac fermion scattering by transverse and longitudinal acoustic phonons in graphene, Phys. Rev. B **100**, 155120 (2019).

[41] O. E. Raichev and M. A. Zudov, Effect of Berry phase on nonlinear response of two-dimensional fermions, Phys. Rev. Res. **2**, 022011(R) (2020).

[42] I. A. Dmitriev, A. D. Mirlin, and D. G. Polyakov, Oscillatory ac conductivity and photoconductivity of a two-dimensional electron gas: Quasiclassical transport beyond the Boltzmann equation, Phys. Rev. B **70**, 165305 (2004).

[43] A. D. Chepelianskii and D. L. Shepelyansky, Microwave stabilization of edge transport and zero-resistance states, Phys. Rev. B **80**, 241308(R) (2009).

[44] S. A. Mikhailov, Theory of microwave-induced zero-resistance states in two-dimensional electron systems, Phys. Rev. B **83**, 155303 (2011).

[45] Y. M. Beltukov and M. I. Dyakonov, Microwave-Induced Resistance Oscillations as a Classical Memory Effect, Phys. Rev. Lett. **116**, 176801 (2016).

[46] See Supplemental Material at http://link.aps.org/supplemental/10.1103/PhysRevB.106.L161408 for a more detailed analysis of the helicity dependence of transmittance, Drude absorption, and MIRO including data measured at different frequencies and the aperture impact on transmittance and MIRO, for the power dependence of MIRO, for the sample design, and for additional details of the measurements.

[47] T. Baba, T. Mizutani, and M. Ogawa, Elimination of persistent photoconductivity and improvement in Si activation coefficient by Al spatial separation from Ga and Si in Al-Ga-As:Si solid system–a novel short period AlAs/n-GaAs superlattice, Jpn. J. Appl. Phys. **22**, L627 (1983).

[48] K.-J. Friedland, R. Hey, H. Kostial, R. Klann, and K. Ploog, New Concept for the Reduction of Impurity Scattering in Remotely Doped GaAs Quantum Wells, Phys. Rev. Lett. **77**, 4616 (1996).

[49] V. Umansky, M. Heiblum, Y. Levinson, J. Smet, J. Nübler, and M. Dolev, MBE growth of ultra-low disorder 2DEG with mobility exceeding 35×10^6 cm^2/Vs, J. Cryst. Growth **311**, 1658 (2009).

[50] M. J. Manfra, Molecular beam epitaxy of ultra-high-quality AlGaAs/GaAs heterostructures: Enabling physics in low-dimensional electronic systems, Annu. Rev. Condens. Matter Phys. **5**, 347 (2014).

[51] G. Abstreiter, J. P. Kotthaus, J. F. Koch, and G. Dorda, Cyclotron resonance of electrons in surface space-charge layers on silicon, Phys. Rev. B **14**, 2480 (1976).

[52] K. W. Chiu, T. K. Lee, and J. J. Quinn, Infrared magnetotransmittance of a two-dimensional electron gas, Surf. Sci. **58**, 182 (1976).

[53] Q. Zhang, T. Arikawa, E. Kato, J. L. Reno, W. Pan, J. D. Watson, M. J. Manfra, M. A. Zudov, M. Tokman, M. Erukhimova, A. Belyanin, and J. Kono, Superradiant Decay of Cyclotron Resonance of Two-Dimensional Electron Gases, Phys. Rev. Lett. **113**, 047601 (2014).

[54] M. L. Savchenko, A. Shuvaev, I. A. Dmitriev, A. A. Bykov, A. K. Bakarov, Z. D. Kvon, and A. Pimenov, High harmonics of the cyclotron resonance in microwave transmission of a high-mobility two-dimensional electron system, Phys. Rev. Res. **3**, L012013 (2021).

[55] L. D. Landau and E. M. Lifshitz, *Electrodynamics of Continuous Media* (Pergamon, Oxford, 1984).

[56] M. Born and E. Wolf, *Principles of Optics: Electromagnetic Theory of Propagation, Interference and Diffraction of Light* (Cambridge University Press, New York, 2000).

[57] E. Mönch, P. Euringer, G.-M. Hüttner, I. A. Dmitriev, D. Schuh, M. Marocko, J. Eroms, D. Bougeard, D. Weiss, and S. D. Ganichev, Circular polarization immunity of the cyclotron resonance photoconductivity in two-dimensional electron systems, Phys. Rev. B **106**, L161409 (2022).